

Solubility and Phase Selection of Copper Tellurates in Alkali Hydroflux

Madalyn R. Gragg 1 Allana G. Iwanicki 2, 3,
Maxime A. Siegler 2, Tyrel M. McQueen 2, 3, 4

1. Department of Physics, Oregon State University
2. Department of Chemistry, Johns Hopkins University
3. Institute for Quantum Matter, William H. Miller III Department of Physics and Astronomy, Johns Hopkins University
4. Department of Materials Science and Engineering, Johns Hopkins University

I. Introduction

Hydroflux synthesis merges two well-established methods of crystal growth: high-temperature fluxes and hydrothermal synthesis [20]. To understand why hydroflux reactions offer unique opportunities within the exploratory synthesis, both hydrothermal and flux systems must be understood. The primary solvent in hydrothermal reactions is H₂O which autodissociates into OH⁻ and H⁺ [20]. These ions assist in the dissolution of reagents which generate in-solution complexes that can undergo precipitation reactions that may generate crystals. On the opposite end of the spectrum, flux reactions are highly ionic species that easily generate A⁺ ions and [OH]⁻ anions that may further dissociate into H₂O and O²⁻ depending on the identity (A) of the hydroxide [5]. By incorporating a roughly equimolar solution of water and (often alkali or alkaline earth) hydroxide heated in a sealed reaction vessel, hydroflux mixtures are basic, oxidizing, low melting reaction environments which can enable formation of distinct products unattainable by either flux or hydrothermal conditions alone. Currently hydroflux synthesis remains relatively underexplored with modern research primarily focused on generating new phases while characterizing their fundamental thermal, magnetic, or optical properties. There is a notable lack of studies addressing the dynamics of H₂O-AOH interactions with reagents in solution and their influence on solid-state formation mechanisms. Understanding these interactions through exploratory synthesis is crucial for the systematic design of materials and their syntheses. Additionally such studies can provide valuable insights on the connections between structure-property and structure-formation relationships, enhancing the construction of materials through rational design.

In this study, we simultaneously investigated and compared two analogous Cu-Te containing phase spaces, Cs-Cu-Te-O(H) and K-Cu-Te-O(H), to explore the synthesis of novel magnetic materials and elucidate the impact of alkali ionic radius and alkali hydroxide dissociation on the hydroflux environment, solubilities of starting reagents, and resulting solid-state incorporation. Additionally, we explored a 1:1 mixed hydroxide phase space, Cs+K-Cu-Te-O(H), to examine how the presence of multiple alkali ions affects product outcome. The K- system was selected due to previous studies that successfully established design trends involving the relative ratios between Cu:Te and H₂O:AOH, which informed the methodology for the Cs- system which is a less extensively studied alkali element. Growth techniques and starting reagents remained constant throughout all reactions and consistent with those performed by A. G. Iwanicki et al [8]. This study focused on a region of phase space where Cu:Te was 1:10 as higher Cu concentrations yielded primarily CuO products in preliminary studies on the Cs- system.

These phase spaces were also selected because of their potential to produce new magnetic oxide phases. Fully oxidized Cu²⁺ has a d⁹ electronic configuration and can act as a model spin 1/2 ion. When ordered in a crystalline lattice, the Cu²⁺ ions can interact and magnetically order based on their relative distances and geometries [8]. Fully oxidized Te⁶⁺ has a full d¹⁰ outer shell and octahedrally coordinates to oxygen, facilitating Cu-Cu magnetic interactions in copper tellurates via superexchange. Partially oxidized Te⁴⁺ exhibits the lone pair effect due to its s² electron pair and has anisotropic coordination which is expected to affect the magnetism in these systems as magnetic pathways may be disrupted or impeded. Furthermore, these phase spaces were evaluated under three distinct levels of reaction environment oxidation, controlled by varying the concentration of H₂O₂ reagent. This allowed for exploration into different regions of phase space across the three systems which were then compared. This allowed us to conclude whether or not the presence of additional oxidizing agents O²⁻ altered the reactions that occurred within the solution environment. More specifically, since hydroflux synthesis is conducted in a closed vessel, this allowed for the incorporation of superoxide and hydroxyl

radicals within the hydroflux reactions. This H₂O₂ study analyzed how the strength of the alkali hydroxide compared to addition of the oxidizing agent, allowing for comparative claims about how CsOH and KOH affected in-solution dynamics

Unique solubility dynamics are present within the Alkali-Cu-Te hydroflux system compared to CuO or TeO₂ in neutral or alkaline environments. Previous research conducted by McDowell et al. and Muller at room temperature have found that the solubility of CuO increases as the [OH]⁻ population increases in alkaline environments using NaOH and KOH, opposite of what is observed in the hydroflux system [9][10]. More modern studies conducted by Navarro M. et al also agree that the population of Cu²⁺ ions with solution scales with [OH]⁻ for LiOH and NaOH highly concentrated alkaline solutions for temperatures up to 60 C but disagree with the magnitude of values reported by McDowell et. al [11]. It has also been determined that CuO is less soluble in neutral solutions than highly basic and acidic solutions in temperatures ranging from 25 to 450 C, implying the presence of H₂O is reducing the solubility of CuO [12][13]. While the solubility of CuO in solutions with varying pH and [OH]⁻ populations has been studied intensively, TeO₂ has not and needs to be in order to better understand the formation of these systems. One study stated that the solubility of TeO₂ is pH dependent and that it is relatively high in acidic or basic solutions whilst minimal in neutral solutions [14]. It was also found that its solubility sharply increases as the temperature increases past 40 C [14].

II. Results

Alkali Ion Dependence For Hydroflux Mixture

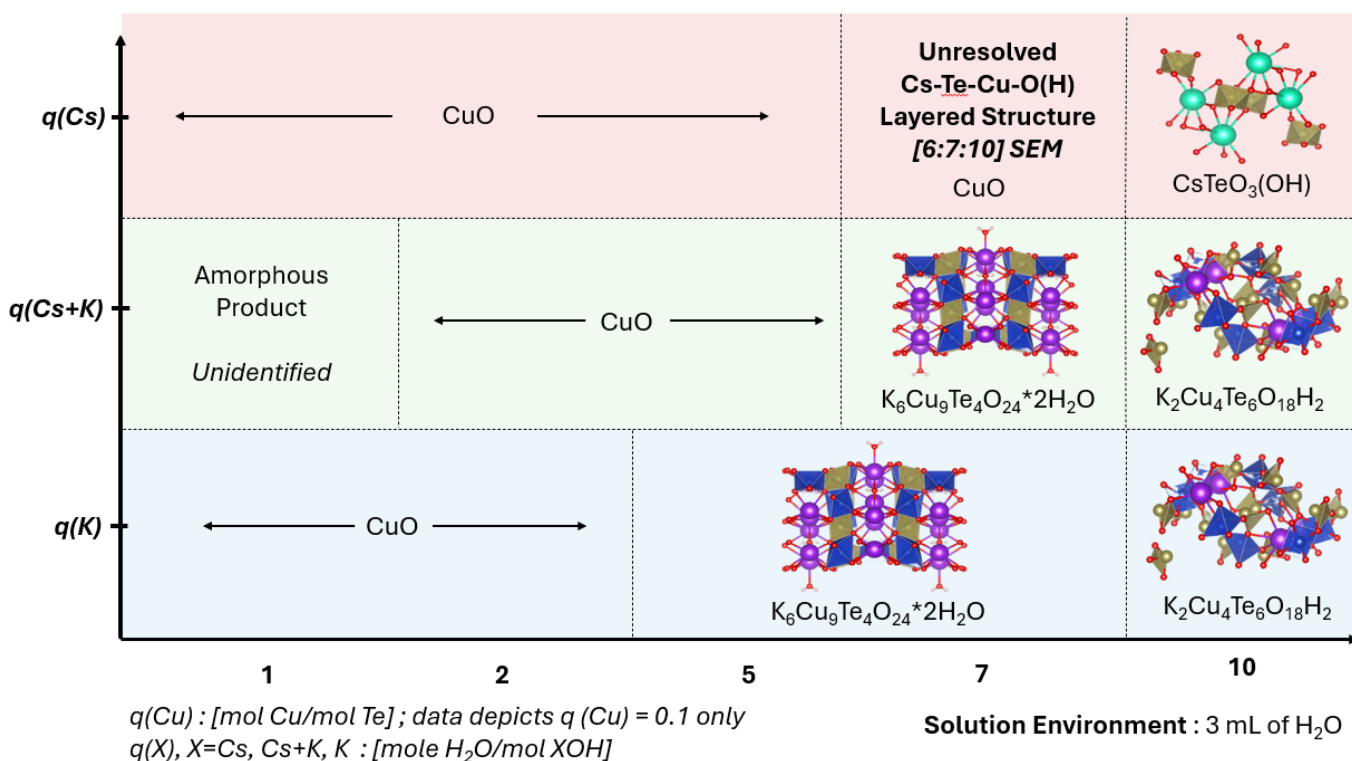
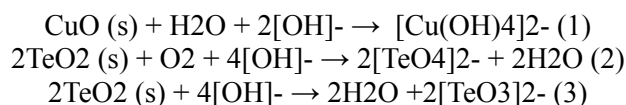


FIG 1: Cs-Te-Cu-O(H), K-Te-Cu-O(H), and 1:1 mixed (Cs+K)-Te-Cu-O(H) phase spaces in the hydroflux environment with no additional oxidizing agents (3 mL H₂O).

The purpose of this work was to investigate the dependence of alkali ionic radius and concentration on the hydroflux properties by characterizing the solid products which precipitate out of three AOH-Cu-Te-O(H) phase spaces, where A = K, Cs, and K+Cs. Since flux behavior of wet hydroxides may depend strongly on available O₂, O₂ present in solution was

varied by testing 0%, 10%, and 30% H₂O₂ aqueous solutions at a range of hydroflux strengths. We then analyzed each product through a reaction equilibrium involving rational intermediate ions in solution as follows.

Reactions which form Te⁴⁺ and Te⁶⁺ products likely involve the distinct intermediates [TeO₃]²⁻ and [TeO₄]²⁻ respectively, with some equilibrium between these two intermediates.[cite] To form [TeO₄]²⁻ from TeO₂ reagent, a redox reaction must occur, so the equilibrium between the two intermediates depends on the concentration of accessible oxidizing species. Since all Cu-containing products contain Cu²⁺ in square planar or similar coordination, [Cu(OH)₄]²⁻ is likely the intermediate Cu ion in solution. Simple formation reactions for these solution intermediates can be seen below in EQ 1 - 3.



From these equations, it can be seen that the solvation of CuO requires both constituents of the mixed H₂O-[AOH] flux, while TeO₂ may be dissolved in the presence of only [AOH], hinting at solubility trends in this system. However, the solubility of CuO in CsOH in this study and in KOH in a previous study vary, suggesting either that these compounds dissociate differently under the reaction conditions, or that a more complicated mechanism of solubilizing CuO occurs, involving the alkali cation.

For all alkali systems in this phase space, the correlation between hydroxide concentration and ratios of Cu and Te in the precipitates suggests that Cu and Te have different solubility trends as a function of hydroxide concentration. At high hydroxide concentration, TeO₂ dissolves fully into solution while CuO reagent can be seen as the majority product; no mixed Cu-Te phases are formed in this region. As the hydroxide concentration decreases, products are formed with Cu:Te = 9:4 for the Cs+K and K spaces and 7:10 in the Cs space, suggesting that Cu and Te complexes are interacting in solution. In the most dilute hydroxide concentrations tested, Cu:Te decreases to 9:4 in the Cs+K and K spaces while the Cs space predominantly yields species with exclusively Te or Cu:Te = 1:2 (resulting from a minority phase CuTe₂O₅). There is an additional correlation between hydroxide concentration, alkali identity, and Te oxidation state in the product. For K-containing systems, intermediate hydroxide concentrations yield Te⁶⁺, while the most dilute hydroxide concentrations yield Te⁴⁺. However, the Cs system yielded Te⁶⁺ even at the most dilute hydroxide concentration, and the mixed system yielded Te⁶⁺ at a more dilute hydroxide concentration than the pure K system. There are two possibilities to consider: that there is less Te⁴⁺ than Te⁶⁺ in solution at higher hydroxide concentration, or alternatively, that the ratios of these intermediates do not change with hydroxide concentration but instead Te⁴⁺ becomes less reactive than Te⁶⁺ towards the Cu intermediate at higher hydroxide concentration.

K- and Cs-K systems may generate similar results while different from Cs- system for several reasons. First, the large ionic radius of Cs⁺ (say number and cite shannons ionic radius table) may prevent it from stably incorporating into the lattice like its smaller analogue K⁺, instead remaining complexes in solution. This may explain a difference between K-containing and non K- containing systems with the same OH⁻ concentration. However, this does not account for the differences within the K and Cs+K phase spaces. This explanation implies that the K ions have more influence on the precipitation reactions within the hydroflux solution and that the Cs ions are likely forming complexes that remain in solution. By itself, this explanation fails to account for the differences between the Cs+K)-Te-Cu-O(H) and K-Te-Cu-O(H). A potential explanation for these dynamics may be caused by the difference in K ion population within the environment as bystander ion concentrations can influence product formation which is further detailed later in results. Additionally, in experiments conducted in open vessels CsOH formed more peroxide and superoxide species than KOH, suggesting a greater oxygen affinity which may actually hinder free O₂ mobility and thus oxidation of Cu and Te in our closed vessel syntheses [5]. Further testing should be performed with a variety of mixed hydroxide phase spaces to reach a more definitive conclusion.

Hydroflux Solution Oxidation Dependence

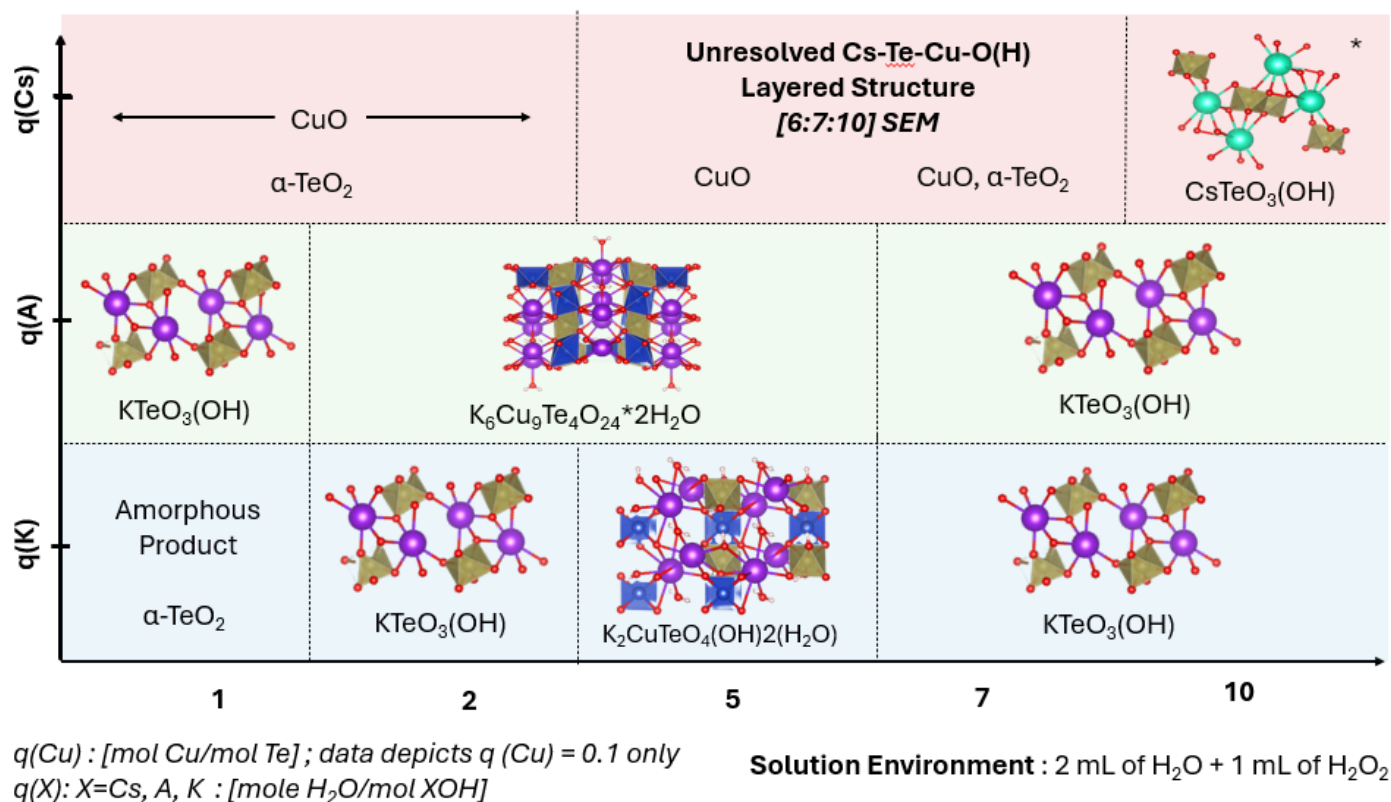


FIG 2: Cs-Te-Cu-O(H), K-Te-Cu-O(H), and 1:1 mixed (Cs+K)-Te-Cu-O(H) phase spaces in the hydroflux environment with no additional oxidizing agents (1 mL and 2 mL H₂O).

To investigate the the dynamics of oxidation potential on the hydroflux solution and the products formed within the Cu-Te-O(H) phase spaces, Cs-, K-, and (Cs+K)- phases spaces at $q(\text{Cu}) = 0.1$ were recreated but with the 3 mL H₂O environment changed to 2 mL of H₂O and 1 mL of H₂O₂, which can dissociate into H₂O and O₂ groups and act as an oxidizing agent. The results of which can be seen in FIG 8. The addition of H₂O₂ had varying effects on the Cs-Te-Cu-O(H), K-Te-Cu-O(H), and 1:1 mixed (Cs+K)-Te-Cu-O(H) phases spaces. The Cs system was minimally affected with primarily differences resulting from the expansion of Layered Cs-Te-Cu into the $q(\text{Cs})$ of 5 region of phase space, the precipitation of alpha-TeO₂ throughout the high and mildly hydroxide concentrated regions, and the removal of CuTe₂O₅ from $q(\text{Cs})$ of 10 region. CuTe₂O₅ is removed from the H₂O and H₂O₂ phase spaces due to the additional O₂ groups reacting to form fully oxidized Te, increasing the population of 2[TeO₄]²⁻ and decreasing 2[TeO₃]²⁻. This is also reflected in how all products formed, independent of alkali identity, have Te+6.

The K and Cs+K systems were heavily altered by the presence of H₂O₂ and seemed to change the phase space entirely, showing that increasing the concentration of lone O₂ groups in the hydroflux solution has an immense impact compared to altering the concentration of hydroxide for medium sized alkali. A new product is observed within this region, KTeO₃(OH), which follows the same series of reactions (EQ 12 - 15) as its Cs analogue. Both systems showed that KTeO₃(OH) reenters the phase space, showing that the phase has a boundary at both a high and low concentration of hydroxide which is referred to as reentrance and is indicative of complex competing solubility trends [18][19]. As seen in the H₂O only phase space, CuO and TeO₂ have inverse stabilities in the hydroflux environment that depends on the

concentration of the hydroxide species and thus the solution's oxidizing potential which heavily implies competing solubility trends which the reentrance of $\text{KTeO}_3(\text{OH})$ confirms. This also shows that $\text{KTeO}_3(\text{OH})$ is the dominant product at two extreme regions, which implies that the increased population of $[\text{OH}]^-$ at highly concentrated hydroxide regions primarily reacts with $[\text{TeO}_4]^{2-}$ as with the increased population of H_2O at low concentrations of hydroxide. In the mildly concentrated region, we instead get intermixing between the Te and Cu intermediates mediated through the near equal population of $[\text{OH}]^-$ and H_2O which appears crucial for the formation of the K products that separate $\text{KTeO}_3(\text{OH})$ regions.

An additional difference between K and Cs+K space is that, unlike in the H_2O only system, the K product formation and its stability depends on the relative amount of K ions in the hydroflux mixture. The Cs+K system was able to produce $\text{K}_6\text{Cu}_9\text{Te}_4\text{O}_{24} \cdot 2\text{H}_2\text{O}$ with reactions $q(\text{Cs} + \text{K})$ of 2 and 5 while the K system created $\text{K}_2\text{CuTeO}_4(\text{OH})_2(\text{H}_2\text{O})$ only with the reaction $q(\text{K})$ of 5. The formation of $\text{K}_2\text{CuTeO}_4(\text{OH})_2(\text{H}_2\text{O})$ requires more K ions than $\text{K}_6\text{Cu}_9\text{Te}_4\text{O}_{24} \cdot 2\text{H}_2\text{O}$ as seen in EQ. An additional difference is that the K only system yielded an amorphous product while the Cs+K phase did not, the inverse of what was observed in the H_2O only system.

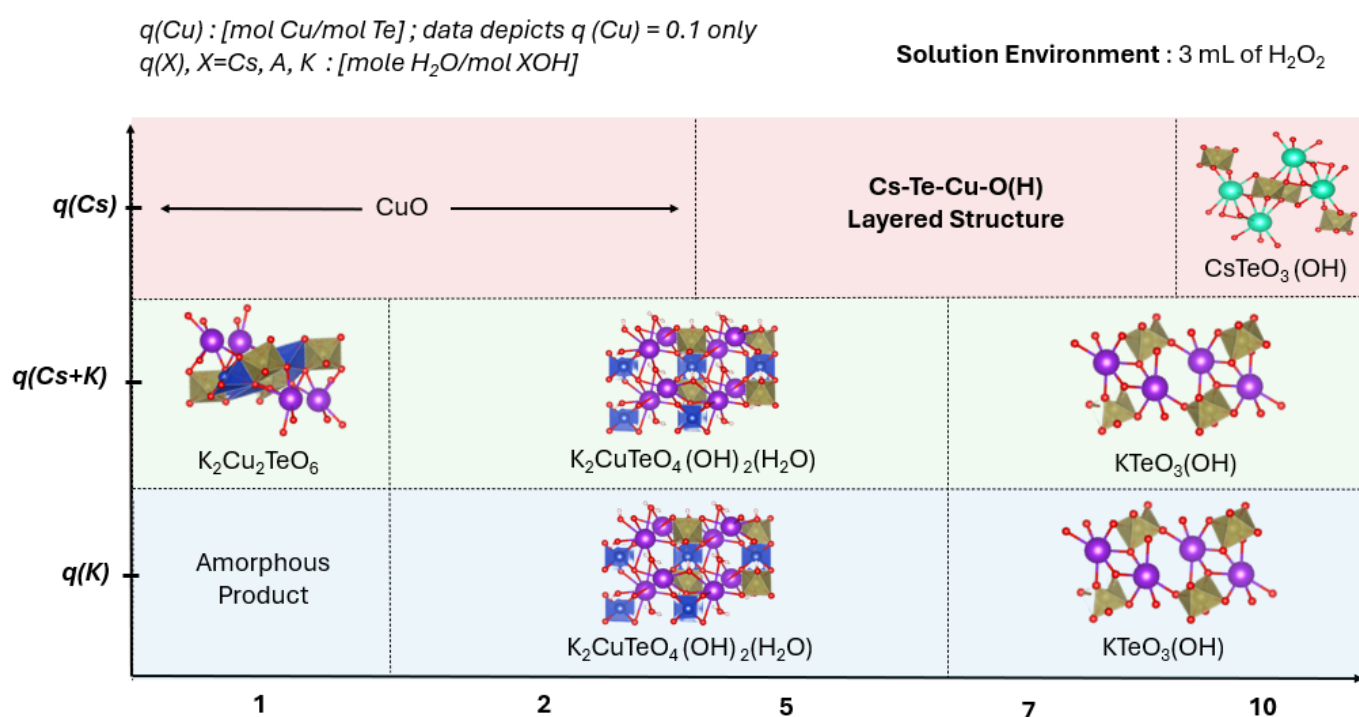


FIG 3: Cs-Te-Cu-O(H), K-Te-Cu-O(H), and 1:1 mixed (Cs+K)-Te-Cu-O(H) phase spaces in the hydroflux environment with no additional oxidizing agents (3 mL H_2O_2).

In order to further quantify the role of the oxidizing agent in these Cu-Te-O(H) systems and the products they form, the phase spaces were recreated with a liquid reagent of 3 mL of H_2O_2 and no H_2O to create a highly oxidizing hydroflux mixture - the results for which is depicted in FIG 9. Again, the Cs-Cu-Te-O(H) system changed minimally from the additional oxidizing agents. The only differences that occurred are that as we move away from the Cu:Te equilibrium is that the formation of $\alpha\text{-TeO}_2$ ceases, as observed in the H_2O only system, while the expansion of Layered Cs-Cu-Te remains. However, the formation of CuTe_2O_5 does not occur, further confirming that the presence of H_2O_2 in the hydroflux mixture eliminates the formation of phases with partially oxidized Te in Cu-Te-O(H) systems. K-Cu-Te-O(H) and Cs+K-Cu-Te-O(H) phase spaces are similar, as seen in the H_2O and H_2O & H_2O_2 systems. The only major difference between the two is that at the highest hydroxide concentration, $q(X)$ of 1, the product $\text{K}_2\text{Cu}_2\text{TeO}_6$ is formed in the Cs+K system and a slightly crystalline but mostly amorphous product is formed in the K system. The products found

within the mild and dilute hydroxide concentrations are the same in the two systems, $\text{K}_2\text{CuTeO}_4(\text{OH})_2(\text{H}_2\text{O})$ and $\text{KTeO}_3(\text{OH})$ respectively. $\text{K}_2\text{Cu}_2\text{TeO}_6$ can be formed using the intermediates $[\text{Cu}(\text{OH})_4]^{2-}$ and $2[\text{TeO}_4]^{2-}$.

$\text{CsTeO}(\text{OH})_3$

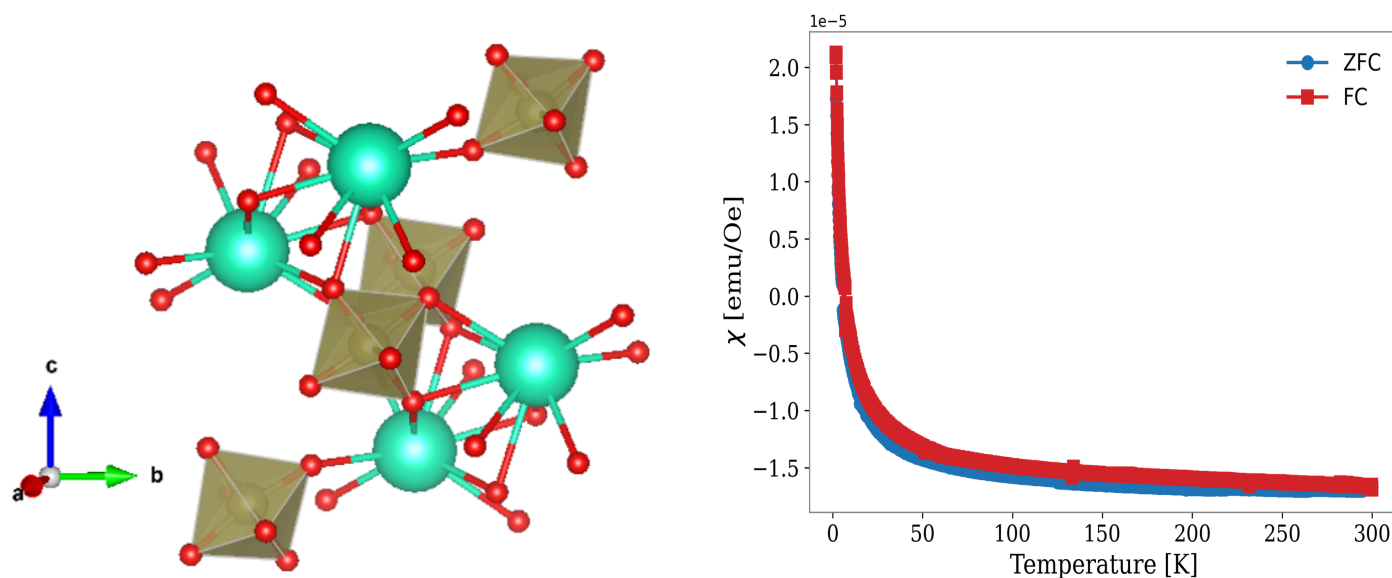


FIG 4: (a) Structure of $\text{CsTeO}_3(\text{OH})$. Outermost TeO_6 octahedra are edge sharing and connect to Cs atoms while the innermost connect to each other. (b) Magnetic susceptibility of $\text{CsTeO}_3(\text{OH})$ measured using ZFC and FC protocols with an external field of $H = 10000$ Oe showing a strong paramagnetic response with insignificant field splitting.

$\text{CsTeO}_3(\text{OH})$ was produced in several reactions, from lowest to highest yield, $q(\text{Cs})$ of 10 with 3 mL of H_2O , 2 mL of H_2O with 1 mL of H_2O_2 , and 3 mL of H_2O_2 . Additionally, $\text{CsTeO}_3(\text{OH})$ was produced using $q(\text{Cs})$ of 7 in the 2 mL of H_2O and 1 mL of H_2O_2 phase space but as a minority phase. $\text{CsTeO}_3(\text{OH})$ formed small, needle-like crystals that were grown either independently or in ball-like clusters. All products of the reactions were mixed-phase, however as the reaction environment became more oxidizing the products became increasingly more pure phase and the yield of $\text{CsTeO}_3(\text{OH})$ increased. For more information regarding what phases were co-produced with $\text{CsTeO}_3(\text{OH})$, please refer to SI. A phase with the same stoichiometry was briefly mentioned in [1] but no structural information was included. Here, we present the synthesis, structure, and magnetic properties of this phase. $\text{CsTeO}_3(\text{OH})$ has two distinct Cs coordinations with minimal structural differences. In both environments, the Cs atoms are coordinated to 9 O atoms. As expected from the large ionic radius of Cs , the overall unit cell volume and alkali-oxygen coordination both are increased relative to other alkali analogues of this phase [2-4]. $\text{CsTeO}_3(\text{OH})$ crystallizes in the space group $P-1$, in contrast to the $P2_1/c$ space group observed in $\text{KTeO}_3(\text{OH})$ and $\text{NaTeO}_3(\text{OH})$. On the opposite extreme of the alkali column, $\text{LiTeO}_3(\text{OH})$ has a space group of $P2_1$ which shows that $\text{CsTeO}_3(\text{OH})$ has the lowest symmetry of the alkali tellurites. This lower symmetry is reflected in its unit cell parameters, where $\text{CsTeO}_3(\text{OH})$ displays 89° - 89° - X angles, diverging from the 90° - 90° - X angles seen in other $\text{ATeO}_3(\text{OH})$ structures [$A = \text{Li}, \text{Na}, \text{K}$]. $\text{CsTeO}_3(\text{OH})$ also has two distinct TeO_6 coordination environments that generate distorted octahedra. One TeO_6 site is edge-sharing while the other is not and heavily deviates from the ideal 90-90 O-Te-O structure.

The fully oxidized states of Te and Cs lead to a lack of strong magnetic ordering due to an absence of lone spins. The only expected magnetic ordering was from weak responses from paired spins in closed orbitals, generating diamagnetic interactions. Despite this, paramagnetic responses were recorded from isolated lone spins as seen in both ZFC and FC χ vs

T measurements in FIG 4. The source of these interactions are either impurities created from generating multiple phases within the reaction's products, such as CuTeO_5 , or broken bonds within a small population of $\text{CsTeO}_3(\text{OH})$ crystals. The expected diamagnetic response was confirmed in isothermal magnetization measurements, also in FIG 2, where at low temperatures the magnetic moments within $\text{CsTeO}_3(\text{OH})$ generate diamagnetic ordering with the applied magnetic field, but paramagnetic interactions at higher temperatures. This also confirms that, despite being a minority phase, the ordering of the impurities is stronger than that of $\text{CsTeO}_3(\text{OH})$ and that the material is weakly magnetic.

$\text{K}_2\text{Cu}_4\text{Te}_6\text{O}_{18}\text{H}_2$

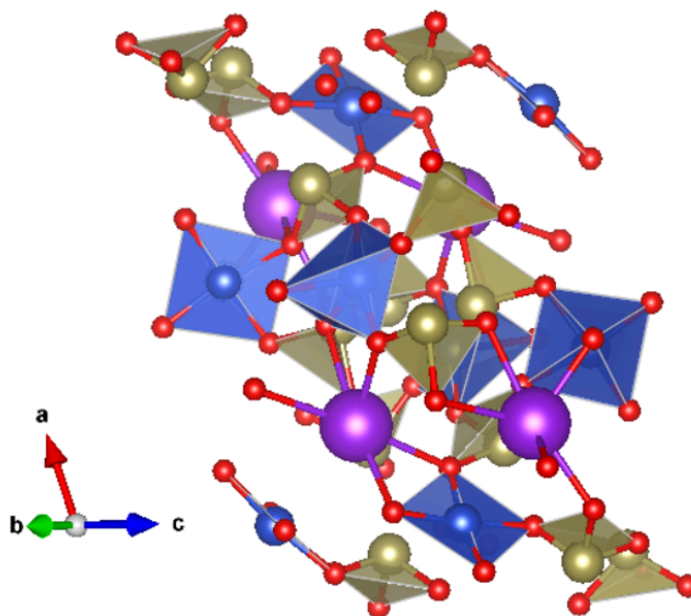


FIG 5: Crystal structure of $\text{K}_2\text{Cu}_4\text{Te}_6\text{O}_{18}\text{H}_2$ (left). CuO_4 square planar plaquettes and CuO_5 square pyramids are linked by Te^{4+} in a distorted coordination due to its lone pair.

$\text{K}_2\text{Cu}_4\text{Te}_6\text{O}_{18}\text{H}_2$, FIG 3, was generated as the majority phase at $q(\text{K}) = 10$, H_2O only, and $q(\text{Cs}+\text{K}) = 10$, H_2O only. Unlike other new phases identified in this work, this reaction product was phase pure and has no other alkali analogues. The three distinct Te^{4+} sites all exhibit the lone pair effect; the lone pairs tend to point towards interstitial sites but bond lengths and angles vary. There are two Cu^{2+} sites, with square planar CuO_4 plaquettes or CuO_5 square pyramids.

Due to the complexity of the Te and Cu coordination environments, magnetic pathways are difficult to fully determine and require DFT modeling or neutron diffraction studies [6-8]. However, ZFC & FC χ vs T and MvH measurements can be used to determine what magnetic ordering and transitions are occurring and their relative strength. As depicted in FIG 4, three magnetic transitions are present, one sharp antiferromagnetic transition at 7 K, where the ZFC/FC splitting is largest, and two possible short range correlations at ~ 22 and ~ 70 K. Isothermal magnetization data depicts possible metamagnetic transitions at $\sim 2\text{T}$ at 2K and 10K.

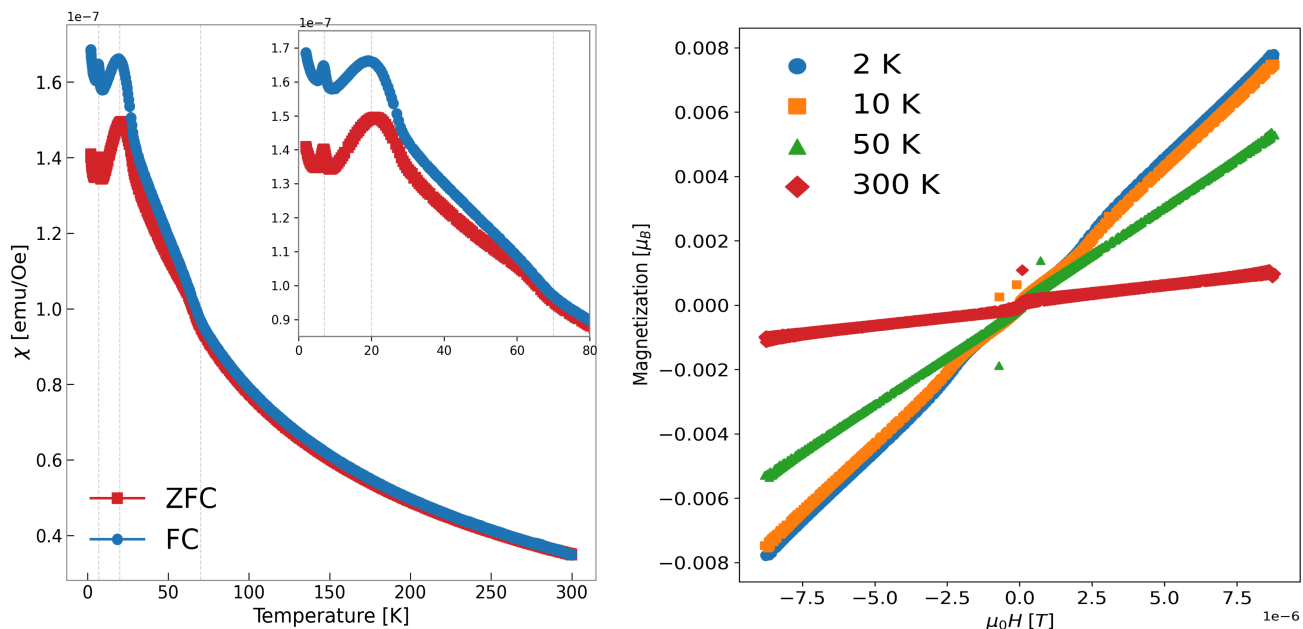


FIG 6: (a) Magnetic susceptibility of $K_2Cu_4Te_6O_{18}H_2$ measured under ZFC and FC conditions with an external field of $H = 10000$ Oe. Three transitions can be seen: two short range antiferromagnetic correlations at $T = \sim 70$ K and $T = \sim 20$ K, and an antiferromagnetic transition at $T = \sim 7$ K. (b) Isothermal magnetization of $K_2Cu_4Te_6O_{18}H_2$ measured at $T = 2, 10, 150$ and 300 K in the range of $\mu_0H = \pm 7$ T applied external field. The $T = 2$ K and 10 K curves show possible metamagnetic transitions at ~ 2 T. Outlier points at low fields are due to instrumental noise.

III. Experimental Methods

Samples were synthesized via hydroflux reactions as follows: powder reagents CuO (Thermo Scientific, 99.995%) and TeO₂ (Acros Organics, 99+%) were combined in the ratio 1:10 with a total quantity of 11mmol. Alkali hydroxides KOH·H₂O (Fisher Chemical 86.6%) and CsOH·H₂O (SIGMA-ALDRICH 90.0%) were combined with DI H₂O and/or H₂O₂ (Fisher Chemical 30%) to achieve molar ratios defined as $q(K) = (\text{moles H}_2\text{O})/(\text{moles KOH}) = 1, 2, 5, 7, 10$, $q(Cs) = (\text{moles H}_2\text{O})/(\text{moles CsOH}) = 1, 2, 5, 7, 10$, and, with equimolar KOH and CsOH, $q(Cs+K) = (\text{moles H}_2\text{O})/(\text{moles KOH} + \text{CsOH}) = 1, 2, 5, 7, 10$. $q(K)$, $q(Cs)$, and $q(Cs+K)$ were calculated assuming anhydrous alkali hydroxide for simplicity. H₂O₂ concentration in aqueous solution was varied at 0%, 10%, and 30% for all systems studied. Reagents were loaded into a 22 mL capacity teflon-lined autoclave with H₂O₂ added last and dropwise to minimize sudden O₂ gas formation. The autoclaves were heated at 200 °C for 2 days in a low temperature oven and quenched to room temperature. Samples were rinsed with DI H₂O and filtered using a vacuum funnel. Single crystal X-ray diffraction (SCXRD) measurements were performed using a SuperNova diffractometer (equipped with Atlas detector) with Mo K α radiation ($\lambda = 0.71073$ Å) under the program CrysAlisPro (Version 1.171.42.49, Rigaku OD, 2020 - 2022). The same program was used to refine the cell dimensions and for data reduction. All reflection intensities were measured at $T = 213(2)$ K. The structure was solved with the program SHELXS-2018/3 and was refined on F 2 with SHELXL-2018/3.[13] Analytical numeric absorption corrections using a multifaceted 3 crystal model were performed using CrysAlisPro. The temperature of the data collection was controlled using the Cryojet system (Oxford Instruments).

Phase purity was determined using powder X-ray diffraction (pXRD) on a Bruker D8 Focus diffractometer equipped with a LynxEye detector using Cu K α radiation ($\lambda = 1.5406$ Å). Data was collected in the range $2\theta = 5-120^\circ$ with a step size of

0.01715° and a step time of 2 seconds. pXRD Rietveld refinements were performed using Topas5 using the refined single crystal structure as the starting point refinement for each compound. Subsequently, only lattice parameters, peak shape, and instrumental zero error were refined and changed from the single crystal solution. Temperature-dependent magnetic susceptibility data was collected on a Quantum Design Magnetic Property Measurement System (MPMS3) from T = 2 - 300 K under an applied field of H = 1000 Oe or $\mu_0H = 1$ T with and without field cooling. Isothermal magnetization measurements were collected at various temperatures with a field range of ± 7 T. All magnetic data were collected on powdered samples. All crystal structure visualizations were done using VESTA.

IV. Conclusions

The results of these studies include the synthesis and magnetic characterization of three novel phases: CsTeO₃(OH), K₂Cu₄Te₆O₁₈H₂, and a Cs-Cu-Te-O layered structure. These products were formed throughout multiple areas within phase space with varying crystal morphologies which is further explained in Results. This study also found that Cs ions in hydroflux reaction environments, independent of solution oxidation, are not likely to incorporate into solid structure and instead remain within solution compared to K ions. This was seen in the lack of variety in product formation for the Cs system and due to K-Te-Cu-O(H) and Cs+K-Te-Cu-O(H) phase spaces producing similar products, implying that the influence of Cs ions was little. Studies generating partitioned, layered materials with 2D magnetism in K-Te-Cu-O(H) show little trend with the Cs- system which only generated one layered structure with weak magnetic ordering. Lastly, this study found evidence supporting that inverse Cu and Te trends exist within these Alkali-Cu-Te-O(H) phase spaces, facilitated through the intermediate products 2[TeO₃]²⁻, 2[TeO₄]²⁻, and [Cu(OH)₄]²⁻. Together, exploratory synthesis and in-solution reaction dynamics elucidated Cu-Te solubility trends not previously reported and allowed for the systematic study of the alkali identity within hydroxide and the effect of additional oxidizers on the hydroflux environment while revealing three new phases.

Funding

The MPMS3 system used for magnetic characterization was funded by the National Science Foundation, Division of Materials Research, Major Research Instrumentation Program, under Grant #1828490. M.G acknowledges REU-Site: Summer Research Program at PARADIM through grant number DMR-2150446.

References:

- [1] Völkl, Hermann, Eder, Felix, Stöger, Berthold and Weil, Matthias. *Zeitschrift für Kristallographie - Crystalline Materials*, vol. 238, no. 1-2, 2023, pp. 7-15. <https://doi.org/10.1515/zkri-2022-0036>
- [2] Ishii, Tsubasa & Shan, Yuejin & Fujii, Kotaro & Katsumata, Tetsuhiro & Imoto, Hideo & Batteredene, Ariunaa & Tezuka, Keitaro & Yashima, Masatomo. (2024). *Dalton Transactions*. 53. 10.1039/D4DT00165F
- [3] Lindqvist O. *Acta Chem. Scand.* 1972, 26, 4107–4120.
- [4] Fujii K , Yoshida Y , Shan YJ , Tezuka K , Inaguma Y , Yashima M . 2020 Sep 7;56(69):10042-10045. doi: 10.1039/d0cc04074f. Epub 2020 Jul 30. PMID: 32729594.
- [5] H. Lux, R. Kuhn, and T. Niedermaier, *Zeitschrift für anorganische und allgemeine Chemie* 298, 285 (1959).
- [6] J. Arul Mary, J. Judith Vijaya, J.H. Dai, M. Bououdina, L. John Kennedy, Y. Song, *Materials Science in Semiconductor Processing*, 34, 2015, 27-38, <https://doi.org/10.1016/j.mssp.2015.02.001>.
- [7] M. Musa Saad H.-E., Ahmed Elhag, *Results in Physics*, 9, 2018, 793-805, <https://doi.org/10.1016/j.rinp.2018.03.055>.
- [8] Allana G. Iwanicki, Brandon Wilfong, Eli Zoghlin, Wyatt Bunstine, Maxime A. Siegler, Tyrel M. McQueen, *Hydroflux-Controlled Growth of Magnetic K-Cu-Te-O(H) Phases*, March 2024, ArXiv

- [9] L. A. McDowell, H. L. Johnston, *Journal of the American Chemical Society (JACS)*. 1936, 57, 2100-2107
- [10] B. Müller, *Z. Physik. Chem.*, 105, 73 (1923).
- [11] Maribel Navarro, Peter M. May, Glenn Hefter, Erich Königsberger, *Hydrometallurgy*, 147–148, 2014, 68-72, <https://doi.org/10.1016/j.hydromet.2014.04.018>.
- [12] Palmer, D.A. *J Solution Chem* 40, 1067–1093 (2011). <https://doi.org/10.1007/s10953-011-9699-x>
- [13] K. I. Shmulovich, B. W. D. Yardley, G. G. Gonchar, *Fluids in the Crust Equilibrium and transport properties*, Springer, 1995, 109 - 114
- [14] Mohammad Mokmeli, David Dreisinger, Berend Wassink, *Hydrometallurgy*, 147–148, 2014, 20-29, <https://doi.org/10.1016/j.hydromet.2014.04.012>.
- [21] R. Albrecht, *Exploration of the Hydroflux*, Phd Thesis, Technischen Universität Dresden (2021).
- [15] Beverskog, B., & Puigdomenech, I. (1995). Studsvik Material AB and Studsvik Eco & Safety AB.
- [16] Bouroushian, M. (Year). Chapter 2: Electrochemistry of the chalcogens. In F. Scholz (Ed.), *Electrochemistry of metal chalcogenides* (pp. 65-69). *Monographs in Electrochemistry*. Springer.
- [17] Filella, Montserrat & May, Peter. (2019). *Environmental Chemistry*. 16. 10.1071/EN19017.
- [18] Raymond E. Goldstein, *J. Chem. Phys.* 83, 1246–1254 (1985)
- [19] T. Narayanan, Anil Kumar, *Reentrant Phase Transitions in Multicomponent Liquid Mixtures*, North-Holland, 1994 - 82 pages
- [20] W. Michael Chance, Daniel E. Bugaris, Athena S. Sefat, Hans-Conrad zur Loye, *Inorg. Chem.* 2013, 52, 20, 11723–11733